ADVANCED ENERGY & SUSTAINABILITY RESEARCH
Open Access
www.advenergysustres.com

Sulfonated Cellulose Membranes Improve the Stability of Aqueous Organic Redox Flow Batteries

*Sanna Lander, Mikhail Vagin, Viktor Gueskine, Johan Erlandsson, Yselaure Boissard, Leena Korhonen, Magnus Berggren, Lars Wågberg, and Xavier Crispin**

The drawbacks of current state-of-the-art selective membranes, such as poor barrier properties, high cost, and poor recyclability, limit the large-scale deployment of electrochemical energy devices such as redox flow batteries (RFBs) and fuel cells. In recent years, cellulosic nanomaterials have been proposed as a low-cost and green raw material for such membranes, but their performance in RFBs and fuel cells is typically poorer than that of the sulfonated fluoropolymer ionomer membranes such as Nafion. Herein, sulfonated cellulose nanofibrils densely cross-linked to form a compact sulfonated cellulose membrane with limited swelling and good stability in water are used. The membranes possess low porosity and excellent ionic transport properties. A model aqueous organic redox flow battery (AORFB) with alizarin red S as negolyte and tiron as posolyte is assembled with the sulfonated cellulose membrane. The performance of the nanocellulose-based battery is superior in terms of cyclability in comparison to that displayed by the battery assembled with commercially available Nafion 115 due to the mitigation of crossover of the redox-active components. This finding paves the way to new green organic materials for fully sustainable AORFB solutions.

1. Introduction

In the efforts worldwide to break our dependency on fossil fuels and switch to renewable energy harvesting alternatives, sustainable energy storage systems will be crucial to achieve success. As many of the renewable energy harvesting systems can only deliver energy intermittently, energy storage is needed to balance demand and grid fluctuations.[1] Several of the most promising technologies for large-scale energy storage, such as redox flow batteries and fuel cells, rely on ion-selective membranes for a proper function. In such systems, the membrane needs to separate fuels or redox molecules in the two cell compartments while allowing the circuit to be closed through efficient ionic transport of, e.g., protons through the membrane. Current state-of-the-art ion-selective membranes, with Nafion as the most prominent example, have severe drawbacks: poor barrier properties toward fuels and redox molecules, environmentally unfriendly production and disposal (noteworthy, a number of EU states are preparing a restriction proposal to cover a wide range of uses of polyfluorinated chemicals[2]), as well as a very high price, which are limiting cost-efficient large-scale application. Due to these issues, there is extensive research activity toward the development of the next-generation ion-selective membranes.[3]

In recent decades, there has emerged an interest in using cellulosic materials for the fabrications of ion-conductive selective membranes, both with cellulose as raw material and as an additive to the membranes based on other materials.[4–6] Other biopolymers such as chitosan and lignin have similarly been investigated as components in the production of novel ionomer membranes.[7–10] Cellulose is of specific interest due to a combination of favorable properties: abundancy as a natural renewable material, low cost, excellent mechanical

S. Lander, M. Vagin, V. Gueskine, M. Berggren, X. Crispin
Laboratory of Organic Electronics
Department of Science and Technology
Linköping University
SE-601 74 Norrköping, Sweden
E-mail: xavier.crispin@liu.se

The ORCID identification number(s) for the author(s) of this article can be found under https://doi.org/10.1002/aesr.202200016.

DOI: 10.1002/aesr.202200016

S. Lander
BillerudKorsnäs Gruvön
SE-664 33 Grums, Sweden

J. Erlandsson, L. Wågberg
Fibre and Polymer Technology
Division of Fibre Technology
KTH Royal Institute of Technology
SE-100 44 Stockholm, Sweden

Y. Boissard, L. Korhonen
BillerudKorsnäs Frövi
SE-718 80 Frövi, Sweden

M. Berggren, L. Wågberg, X. Crispin
Wallenberg Wood Science Centre
Fibre and polymer Technology
KTH Royal Institute of Technology
SE-100 44 Stockholm, Sweden

properties, an ability to form networks at different size ranges and high possibilities for various chemical functionalization routes. Cellulose is a biopolymer with abundant hydroxyl groups along the polymer chains, readily available for chemical modifications, for example, the introduction of cationic or anionic functional groups.[11,12] Cellulose has already been successfully used in energy storage systems in different ways: as porous separators for metal-ion batteries,[13] as ion-selective membranes in inorganic redox flow batteries,[14] as electrodes by its combination with conducting materials,[15] and as proton conducting membranes for fuel cells.[16] However, a recent review[17] concluded that proton conductivity of cellulose itself was insufficient for energy storage applications, so that introduction of acidic groups by chemical modification of cellulose would be a promising route. Indeed, membranes prepared from cellulose nanocrystals produced by sulfuric acid hydrolysis have been found to possess excellent proton conductivity due to the residual sulfate ester groups on the cellulose nanocrystal surfaces.[14,16]

An idea naturally arising from these observations is to find a way to modify cellulose chemically to incorporate a higher density of sulfonic acid groups. At the same time, for use in aqueous environments of many redox flow battery systems, wet stability of the membranes is essential and can be obtained by cross-linking of the cellulose. Importantly, there exists a two-step modification route for cellulose that incorporates both sulfonic acid groups and aldehydes into the cellulose structure, the latter capable of forming inter- and intramolecular cross-links via hemiacetals.[18–20] This functionalization of cellulose has previously been studied in a different context: as a prehomogenization processing step, it indicates an economic advantage due to lowered energy demand in the material production.[21] Oxidatively sulfonated cellulose has also been proposed for other uses, for example, as an immunosorbent[22] and as a dispersion agent.[23] The same functionalization route has been used with bacterial cellulose as starting material in combination with polyaniline to prepare composite membranes for fuel cell applications.[24] Recently, Bayer et al. used oxidatively sulfonated cellulose nanofibrils to produce membranes for fuel cells, and were able to achieve a high power density of 160 mW cm^{-2} by using spray coating to produce thin membranes from the material, thus decreasing the resistance of the device.[25]

In this study, fully bleached cellulose fibers were subjected to the sequential oxidation and sulfonation (**Scheme 1**) to graft both cross-linking and ionic-selective functionalities (**Scheme 2**). The modified fibers were subjected to high-pressure homogenization to produce nanofibrils from which membranes were produced. The fabricated membranes showed excellent homogeneity, low porosity, and stability in aqueous environment originating from the cross-linking of aldehyde groups.[26] Characterization of our membranes with a number of physicochemical methods revealed narrow nanochannels and high water content. We believe that it is this combination of properties that leads to the enhancement of barrier properties of the sulfonated cellulose membranes toward ionic redox compounds in comparison with Nafion 115, which resulted in the cycling stability improvement of the model aqueous organic redox flow battery (AORFB). Crossover of active species in flow batteries is a complex phenomenon governed by several transport mechanisms such as diffusion, migration, and convection, in particular electroosmotic drag. The crossover flux from each mode of transport depends on fundamental properties of the membrane, and it is not straightforward to experimentally determine the contributions of each mode to the total crossover flux. As an example, results from diffusion permeability tests may in some cases not correspond well to the actual performance of the flow battery system.[27] In our case, we believe that it is electroosmotic drag that was especially reduced.

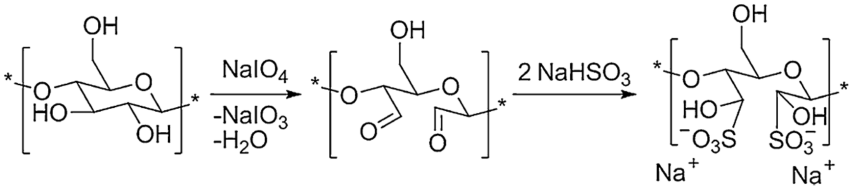

Scheme 1. Regioselective oxidation of the C2—C3 bond of the cellulose anhydroglucose unit by sodium periodate, followed by sulfonation of the aldehyde groups by sodium bisulfite.[8]

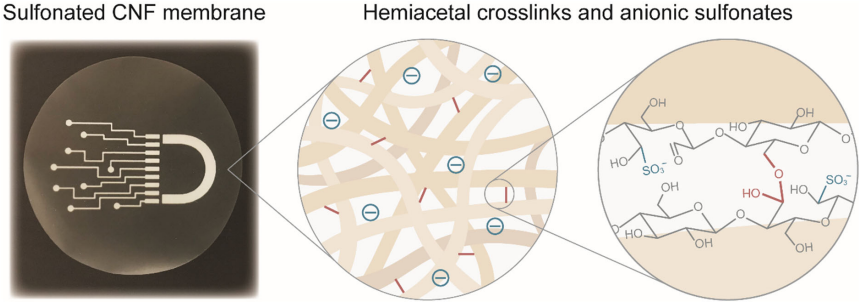

Scheme 2. Visualization of the dual functionality obtained by the chemical modification of the starting material: cross-links between fibrils due to formation of hemiacetals and fixed anionic sulfonates on fibril surfaces.

2. Results and Discussion

2.1. Modification and Homogenization of Cellulose Fibers

The aldehyde content of the pulp after periodate oxidation quantified by the alkaline titration of hydroxylamine reaction mixture was 1.2 m mol g^{-1}, corresponding to a degree of oxidation of approximately 10% of the anhydroglucose units. The sulfonate group content measured as total charge by conductometric titration on oxidized pulp after sulfonation was 0.34 m mol g^{-1}. The incomplete aldehyde-to-sulfonate conversion implies the preservation of 75% of residual aldehyde groups available for further cross-linking assuring the structural stability under wet conditions. The lower limit for good wet stability has previously been found to be around 0.6 m mol g^{-1} of aldehydes in similar systems.[26]

The processing of the sulfonated pulp to the gel form of nanofibrils was achieved by the high-pressure homogenization (passing the fibers through 200 and 100 µm microfluidics chambers at a pressure of 1500 bars). The low number of necessary passes through the homogenizer illustrates the favorable modification route[21] accomplishing lower energy demand for the cellulose nanofibril production.

2.2. Membrane Preparation, Surface Morphology, and Mechanical Properties

The membranes prepared from the sulfonated and fibrillated cellulose by means of vacuum filtration were free-standing, homogeneous, transparent, and could be easily peeled off from the filters (**Figure 1**A). The membranes were fully intact after 1 week storage in water, thus showing excellent wet stability achieved by the cross-linking of created aldehyde groups.

The sulfonated and fibrillated cellulose membranes in dry state showed tensile strengths of 187 ± 25 MPa, strain at breaks of 4.3 ± 1.6%, and Young's moduli of 10.0 ± 0.6 GPa (Figure S4, Supporting Information), which is comparable to previously reported values for films made from nanofibrillated cellulose.[28] Therefore, the utilized chemical modification does not significantly affect the mechanical properties of cellulose membranes.

The tensile properties of the membranes in wet state were also investigated, showing a reduced tensile strength of 23 ± 2 MPa, an increased strain at break of 17.9 ± 2.0%, and a Young's moduli of 0.43 ± 0.01 GPa (Figure S4, Supporting Information). These values are comparable to those reported for Nafion membranes measured in wet state,[29] indicating that while the strength of the cellulose membranes is not as excellent in the wet state as in the dry state it is still most likely sufficient for the intended applications.

Both atomic force microscopy (AFM) (Figure 1B) and scanning electron microscopy (SEM) (Figure 1C,D, S1, S2, Supporting Information) revealed an asymmetry in morphology of the dried, different sides of the membrane. The contact with the filter during vacuum filtration yielded the appearance of irregular structures with the size of a few micrometers distributed over the smooth surface (Figure 1C and S2, Supporting Information). Closely packed structures with sizes in the nanometer range (Figure S3, Supporting Information) were observed in the smooth regions of the membranes, indicating that the

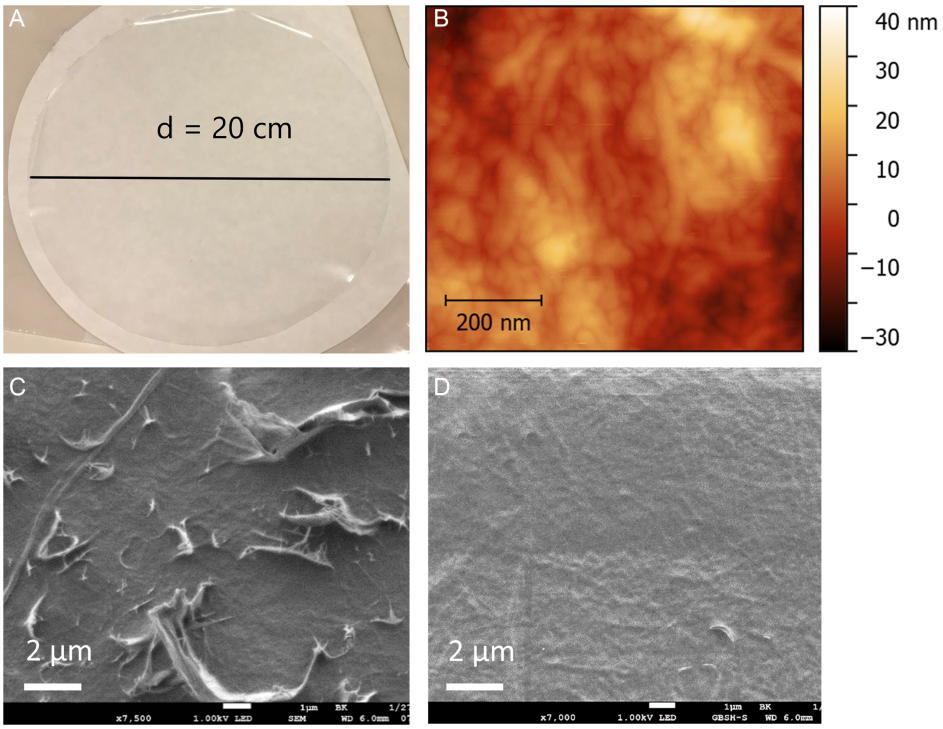

Figure 1. Sulfonate cellulose membranes. A) Photograph; B) AFM image; C,D) SEM images of membrane sides in contact and without contact with filter during vacuum filtration.

cellulose nanofibrils were densely packed creating a structure with pore sizes in the nanometer range.

Elemental analysis by EDS of the membrane surface showed a sulfur content of approximately 0.25 wt%, indicating that sulfonate groups are indeed present in the membranes prepared from the sulfonated cellulose nanofibrils (Figure S2E, Supporting Information).

2.3. Porosity

Three samples were cut from the single membrane of sulfonated cellulose and evaluated with liquid–liquid displacement porometry using isobutanol and water as wetting and displacement liquids, respectively.[30] No flow was detected up to a maximum pressure of 35 bar for two samples, indicating an average pore size below 2 nm (Figure S5, Table S1, Supporting Information). The flow at approximately 20 bar was detected for the third sample, corresponding to an average pore size of 4 nm, which is probably due to the presence of an irregular defect or pinhole. In coherence with microscopy data, the porometry shows that the sulfonated cellulose membranes are dense, which controls their barrier properties toward aqueous solutions and large molecules. Additionally, the membranes were subjected to pressures of up to 35 bar without showing signs of damage, indeed showing their robustness. The membrane porosity was also studied by nitrogen sorption (BET). The obtained results (Figure S6, Supporting Information) show a low surface area of around 2 $m^2 g^{-1}$ as well as an almost zero pore volume, again demonstrating the low porosity of the membranes.

2.4. Ionic Transport properties

To compare the ionic transport characteristics in the membranes of sulfonated cellulose and Nafion, both dynamic and steady-state measurements were performed using aqueous electrolyte. The four-probe setup (upper inset in **Figure 2**A) was used for the linear sweep voltammetry as a dynamic measurement for the equilibrated membranes in 0.5 M KCl. Ionic conductivity was calculated according to

$$\sigma = \frac{L}{R_{\text{membrane}} * A} \tag{1}$$

where L is the membrane thickness (m); R_{membrane} is membrane resistance ($R_{\text{membrane}} = R_{\text{total}} - R_{\text{contact}}$, where R_{total} and R_{contact} are measured resistances (Ω) of the cell with and without the membrane, respectively). R_{contact} measured without membrane actually includes both the electrolyte resistance between electrode and membrane, and the electrical contact resistance at the electrode. A is the active area of membrane during measurement (m^2). In the case of sulfonated cellulose, the measurements of R_{total} were carried out on stacks of one, two, and three membranes. The extrapolation to the zero thickness (lower inset in Figure 2A) yielded R_{contact}. Showing a good reproducibility, the ionic conductivity of sulfonated cellulose was evaluated with respect to the total thickness stack (Supporting Note 1).

The ionic conductivities of sulfonated cellulose and Nafion 115 in 0.5 M KCl were 11.2 ± 0.6 and 11.9 mS cm^{-1}, which is quite close and implies the comparable characteristics of the

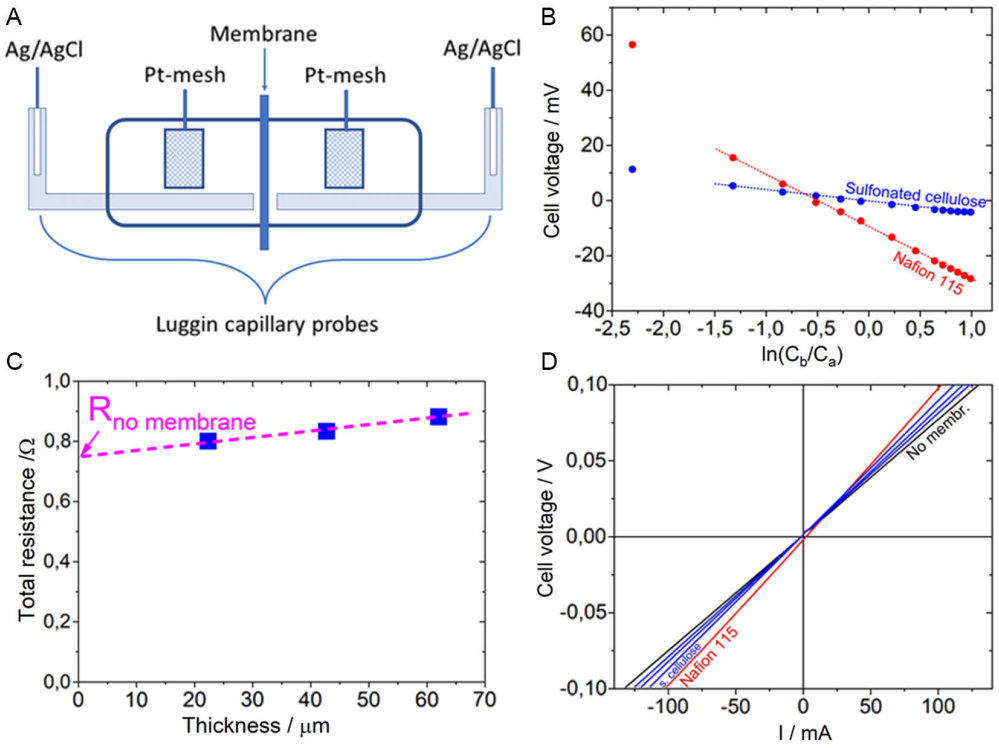

Figure 2. Membrane ionics on sulfonated cellulose (blue) and Nafion 115 (red) in aqueous KCl. A) Schematic of the membrane H-cell used for ionic transport measurements. B) Diffusion potentials. C) Thickness dependence of the total resistance for sulfonated cellulose membrane. D) Linear sweep voltammetry.

dynamic ionic transport. The ionic conductivity of the membranes was additionally evaluated in 0.1 m H_2SO_4 using the same method as described above. The values obtained were 5.2 ± 1.2 and 23.5 mS cm^{-1} for sulfonated cellulose and Nafion 115, respectively, demonstrating the excellent proton conductivity of Nafion. The absolute ionic conductivities obtained from measurements of membrane resistance are strongly dependent on the method and experimental conditions used,[31] which may explain the lower values of conductivity of Nafion compared to what is often reported in the literature.

To compare the ionic selectivity, as a preference for the membranes to discriminate the transport of either anions or cations under conditions of thermodynamic equilibrium, the measurements of concentration cell potentials in aqueous KCl were performed. Transport numbers were obtained from the linear slope of the cell potential plotted as a function of $\ln(C_b/C_a)$ (Figure 2B)[32]

$$E = (t_- - t_+)\frac{RT}{F}\ln\frac{C_b}{C_a} \tag{2}$$

where E is the measured cell potential (V), t_+ and t_- are the transfer numbers for cations and anions, respectively ($0 < t < 1$, $t_+ = 1 - t_-$), C_b and C_a are the concentrations of anions and cations, R is the gas constant (8.3145 mol^{-1} K^{-1}), T is an absolute temperature (K), and F is a Faraday constant (96485.3 A s mol^{-1}). The slope $m = E * \ln\frac{C_a}{C_b}$ corresponds to $(t_- - t_+)\frac{RT}{F}$. The transport numbers can be obtained as

$$t_\pm = \frac{1}{2}\left(1 \mp m \cdot \frac{zF}{RT}\right) \tag{3}$$

where z is the charge number of ions. The transport numbers of cations (t_+) were 0.87 and 0.58 for Nafion 115 and sulfonated cellulose membranes, respectively. The transport numbers of anions (t_-) were 0.13 and 0.42 for Nafion 115 and sulfonated cellulose membranes, respectively. The significantly higher transport number of cations illustrates the general selectivity for cation transport obtained on both membranes. The transport numbers of sulfonated cellulose membranes demonstrate but a moderate improvement over those characteristics for 1 M KCl solution ($t_+ = 0.49$ and $t_- = 0.51$), thus illustrating their rather weak selectivity toward cation transport, clearly behind Nafion 115 in this respect. These results are, however, not surprising considering the much higher density of negatively charged groups in Nafion 115 compared to the sulfonated cellulose membranes.

Additionally, transport numbers for protons in the membranes were studied by measuring concentration cell potentials in H_2SO_4. For this purpose, H_2SO_4 was treated as fully dissociated and the proton transport numbers were obtained from the equation for the cell potential for a 1:2 electrolyte[33]

$$E = -\left(\frac{1}{2} - \frac{3}{2}t_+\right)\frac{RT}{F}ln\frac{a_b}{a_a} \tag{4}$$

Activity coefficients for H_2SO_4 at the relevant concentrations were obtained from the literature.[34] The proton transport numbers (t_+) calculated from the cell potentials were 0.98 and 0.93 for Nafion 115 and sulfonated cellulose membranes, respectively. Taking into account that the proton transport number in H_2SO_4 solution (t_e) is 0.82,[35] that is quite high, the new sulfonated cellulose membrane still shows improvement over this value. Decisively, the low porosity membranes with an ability to prioritize the transport of a certain type of ions while having a barrier property for their counter-ions and the rest of the chemical composition is of high technological importance. Specifically, the proton transport on ion-selective membranes is essential in most of the chemical-to-electrical energy conversion technologies such as fuel cells and redox flow batteries. Limiting the rate of the whole process, the proton transport on proton-exchange membrane (PEM) is fast and attributed with a barrier property, which maintains the electrical energy gradient by the suppression of chemical cross-contamination. Therefore, the low porosity ion-selective membranes have an essential advantage over the porous physical separators.

The permselectivity, that is a measure of ability of the membranes to discriminate between anions and cations, can be calculated according to[36]

$$P = \frac{(t_+ - t_e)}{(1 - t_e)} \tag{5}$$

The permselectivity thus obtained is 0.89 for Nafion 115 membrane and 0.61 for sulfonated cellulose membrane, demonstrating that while both membrane types possess proton selectivity, Nafion 115 is superior to the sulfonated cellulose membrane in this respect.

The permselectivity obtained for the sulfonated cellulose membrane is higher in H_2SO_4 (0.61) compared to KCl (0.18). This indicates more efficient proton transport compared to other cations in the cellulose membrane, plausibly owing to the abundancy of both $-OH$ and $-SO_3$ groups in combination with the small pore size. The high water content of the sulfonated cellulose membranes may facilitate proton transport by the Grotthus mechanism, in which protons can hop between water molecules via the formation and cleaving of hydrogen bonds.[16]

2.5. AORFB Performance

Having characterized the membranes themselves, we now compare the behavior of a model AORFB device, in which they are used. As the development and optimization of an organic redox system are not the objective of this work, we chose a known and accessible pair of compounds among quinones, widely studied in the AORFB context though we are aware of their intrinsic problems that lead to capacity fading.[37] Our AORFB is based on alizarin red S and tiron solutions as anolyte and catholyte (**Figure 3**A), respectively. Alizarin red S has a redox potential of -0.08 V (vs AgCl/Cl) and tiron has a redox potential of 0.69 V (vs AgCl/Cl);[38] hence the expected open-circuit potential of the redox flow cell should be 0.77 V. We compare the behavior of commercial Nafion 115 (thickness 127 μm) and our sulfonated cellulose (thickness 20 μm) membranes as selective membranes in the same AORFB architecture with this redox pair. The values of cell resistances estimated by high frequency impedance measurements were similar for both systems (Figure S8, Supporting Information).

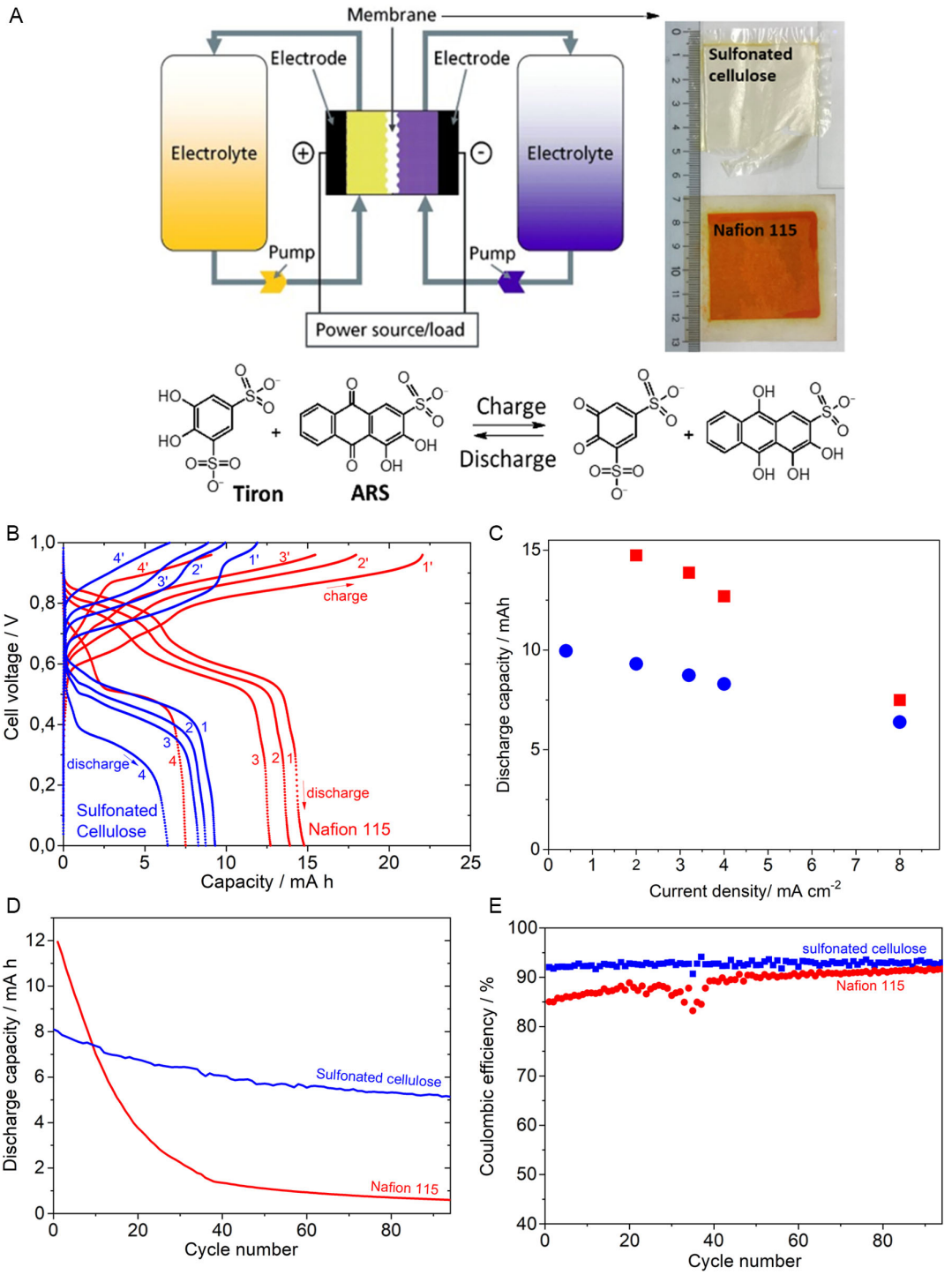

Figure 3. The improvement of AORFB functional stability by sulfonated cellulose membrane (blue curves) in comparison with Nafion 115 (red curves). A) Working principle, redox chemistry of AORFB, and visual appearance of alizarine red S in the bulk of Nafion 115 membrane after AORFB cycling. B) Cell voltage versus capacity plots at current densities of ± 2.0 mA cm^{-2} (1, 1'), ± 3.2 mA cm^{-2} (2, 2'), ± 4.0 mA cm^{-2} (3, 3'), and ± 8.0 mA cm^{-2} (4, 4') mA cm^{-2}. C) The discharge capacity retention. D,E) The evolutions of discharge capacity (D) and coulombic efficiency (E) with GCD cycling.

Galvanostatic charge–discharge characteristics (GCD) at 4 mA cm^{-2} resulted in similar initial performance output (Figure S9, Supporting Information), though the sulfonated cellulose membrane showed somewhat lower discharge voltage (Figure 3B). The increase of GCD currents (from 0.4 to 8 mA cm^{-2}) led, as usually, to the decrease of stored electrical

charge capacity more pronounced on Nafion than on the sulfonated cellulose membrane (Figure 3C), such that similar device characteristics with the two membranes were observed at a high discharge current of 8 mA cm^{-2}.

The continuous GCD cycling at intermediate 4 mA cm^{-2} showed higher capacity retention observed for the sulfonated cellulose-based AORFB in comparison with Nafion-based device (Figure 3D, S10, S11, Supporting Information), after a just few (less than 5) initial cycles during which Nafion outperforms sulfonated cellulose membrane (Figure 3D): after 90 cycles, the cellulose-based membrane allows to retain 63% of capacity retention, versus only versus 5% with Nafion. Moreover, in contrast to sulfonated cellulose-based AORFB performance, the coulombic efficiency of Nafion-based device was significantly lower than 100% from the very beginning (Figure 3E). These observations indicate that the crossover of redox components is the major cause to the degradation for AORFB based on Nafion 115. Part of the current used in the Nafion-based device was spent on a side reaction (e.g., electrode reactions of contaminants transferred by crossover) that lowers the coulombic efficiency. The drop in capacity on Nafion-based device (Figure 3E) illustrates the electrolyte starts to be depleted of redox species, by crossover, and the AORFB becomes exhausted (Figure S9, Supporting Information). High coulombic efficiency observed with Nafion at high cycle numbers can, curiously, be related to the same deterioration, as the contribution of constant capacitive storage increases with respect to fading faradaic storage.

The lower crossover of alizarine red S through the sulfonated cellulose in the AORFB was evidenced by a significantly less intensive color of the membrane after the overnight cycling (inset in Figure 3E) in comparison with Nafion 115. The Nafion 115 was completely orange, indicating that a significant amount of alizarin dyes penetrated in the membrane. We hypothesize that this observed uptake of the dye in Nafion is due to the amphiphilic character of the alizarin red S, leading to its penetration into the hydrophobic fluorinated nanodomains.[39] The attenuated total reflectance Fourier transform infraRed spectroscopy (ATR-FTIR) analysis (Figure S12, Supporting Information) of sulfonated cellulose membrane showed no distinct changes in the spectra upon AORFB operation, indicating its sufficient chemical stability to withstand the environment of the AORFB. In contrast, a novel peak (at ≈969 cm^{-1}) was observed for Nafion after the device operation. This peak may be due to the hydration state of the membrane, as the peak at ≈970 nm^{-1} is associated with electrostatic and hydrophilic interactions that affect the $-SO_3^-$ groups during membrane hydration.[40,41] No peaks that could be assigned to the redox molecules in the AORFB electrolytes were detected in the Nafion membrane, despite its strong orange color.

It has been demonstrated that a leading factor of the crossover of the redox components under RFB operation is electroosmotic drag,[27] a transport mechanism in which the redox components move in association with solvent molecules that are dragged along with the current of ions through the membrane. In this case, high water content in a membrane has a known effect to inhibit such crossover. We, therefore, studied the water uptake (WU) by both membranes and estimated it for sulfonated cellulose membranes to ≈200%, while only ≈25% for Nafion 115 (Table S3, Supporting Information). This agrees with the hypothesis of higher water content being the key to curbing crossover with our cellulose-based membranes. Looking for the reason for much higher WU in the sulfonated cellulose membrane compared to Nafion, we suppose that it is the presence of hydrophilic moieties (hydroxyl and sulfonic acid groups) in cellulose and the absence of hydrophobic fluorocarbon domains found in Nafion, could both contribute.

3. Conclusion

A novel class of membrane has been prepared from nanofibrillated cellulose of wood origin via periodate/bisulfite processing and characterized with respect to surface morphology, mechanical properties, porosity, and ionic transport phenomena. The advantages of the sulfonated cellulose as a starting material for membranes in electrochemical devices include inexpensive raw material, straightforward membrane production route, and the mitigation of the crossover inherent to the state-of-the-art commercial ion-selective membranes.

The ionic conductivity of the novel membrane in 0.5 M KCl was 11 mS cm^{-1}, the same as for Nafion115, while in 0.1 M H_2SO_4 it was about 5 mS cm^{-1} 4 times lower compared to Nafion. Ionic selectivity of our sulfonated cellulose membranes, according to the transport numbers we measured in KCl and H_2SO_4, was higher for proton transport compared to other cations. This observation indicates the applicability of this novel membrane type in systems based on proton transport coupled with selectivity.

We integrated the sulfonated cellulose membrane in a model quinoid AORFB based on organic quinones in acidic electrolytes, i.e., where proton transport is desired. Specifically, we choose for this proof-of-concept alizarin red S as negolyte and tiron as posolyte.

In all, this first cellulose-based membrane separator for AORFB system largely outperformed commercial Nafion 115 membrane in terms of device functional stability, as evidenced by 63% versus 5% capacity retention after 90 cycles. Visibly, the cellulose membrane does not change its aspect after cycling, while Nafion takes on a strong orange color, which indicates that the latter membrane is not impermeable for the dye.

Although this behavior might be specific to those dyes, the chosen dyes represent typical quinoid AORFB redox systems under extensive study. We attribute the improvement in stability to the inhibition of crossover of the redox species in the anolyte and catholyte. Among various transport mechanisms (diffusion, migration, electroosmotic drag), we suggest the effect is primarily due to the suppression of electroosmotic drag, inversely related to water content in the membrane.

The sulfonated cellulose membranes with inherent crosslinking obtained via chemical modification presented herein are proposed as a new template for a next generation of cheap and green selective membranes specifically designed for use in aqueous electrolyte systems such as redox flow batteries.

4. Experimental Section

Materials: A fully bleached softwood pulp from SCA (K46) was used. All chemicals (sodium metaperiodate, sodium metabisulfite, hydroxylamine

hydrochloride, sodium hydroxide, sodium chloride, alizarin red S, tiron, sulfuric acid) were purchased from Sigma-Aldrich and used as received. Laboratory filter papers were obtained from Ahlström-Munksjö, grade 5 for pulp wash and grade 1001 for fiber dry weight determinations. In the redox flow battery, carbon paper (AvCarb MGL 190, FuelCellStore (TX, USA)) was used as electrodes, graphite felt (AvCarb G200 FuelCellStore (TX, USA)) was used as diffusion layer, and Nafion 115 membranes were purchased from Sigma-Aldrich and used after activation according to a standard prescribed procedure.[42] Deionized water was used throughout all experimental procedures.

Oxidation and Sulfonation of Cellulose: A fiber dispersion of 20 g L^{-1} in water was prepared. Sodium periodate was added in a mass ratio 1.35:1 to the pulp. The reaction was performed in darkness under stirring at 200 rpm for 30 min at 50 °C. Isopropanol at 6.3 wt% was then added as a radical scavenger. The oxidized fibers were washed thoroughly with deionized water.

A dispersion of the oxidized fibers was then prepared at 20 g L^{-1} in deionized water. The sulfonation was then performed by adding sodium metabisulfite in a mass ratio 0.3:1 to the oxidized pulp. The reaction was performed at room temperature under stirring at 400 rpm for 2 h. The sulfonated fibers were washed thoroughly with deionized water.

Homogenization of Sulfonated Cellulose: A microfluidizer M110EH Microfluidics (MA, USA) was used to homogenize the sulfonated fibers. The fiber suspension was first run one time through a set of chambers of 500 µm and 400 µm channel diameters, respectively, in series, and subsequently 4 times through a set of chambers of 200 and 100 µm channel diameters, respectively, in series. The pressure was kept at 1500 bar during all operations.

Film Preparation: To fabricate films from the homogenized sulfonated fibers, a vacuum filtration technique was used as a first step for dewatering. Durapore DVPP membranes from Merck Millipore with a pore size of 0.65 µm were used for the filtration. Fibril dispersions in deionized water at a concentration of 0.1% were prepared and stirred overnight with magnetic stirrer prior to film fabrication. After dewatering, the films were dried by hot-pressing at 93 °C using the drying section of a Rapid Köthen sheet former (Paper Testing Instruments, Pettenbach, Austria).

Larger films for device tests were fabricated using a Rapid Köthen sheet former. Durapore DVPP membranes from Merck Millipore with a pore size of 0.65 µm were cut to the correct size for the sheet former from a roll of the material. The Rapid Köthen dewatering section was run at its maximum vacuum pressure of approximately 1 bar to dewater the films. The films were dried by hot-pressing at 93 °C using the Rapid Köthen drying section.

The thickness of the produced films was measured with an L&W Micrometer (ABB Lorentzen & Wettre, Sweden), with a precision of 0.1 µm.

Aldehyde Content Determination: The content of aldehyde groups was estimated after the oxidation of cellulose fibers by the reaction with hydroxylamine followed by the titration of stoichiometrically released proton by sodium hydroxide.[43] The suspension of 0.1 g of dry oxidized cellulose in 25 mL of water was prepared. The pH values of oxidized cellulose suspension and hydroxylamine solution (concentration) were lowered to 4 by 0.1 M HCl. Hydroxylamine solution (25 mL) was added to each of the cellulose suspensions. The reaction was left to proceed for 2 h at room temperature. Then the solutions were titrated back to pH 4 using 0.1 M NaOH. The number of moles of NaOH consumed was used to calculate the corresponding amount of aldehydes in the sample. This amount was then normalized with respect to the exact dry weight of the sample fibers as determined by filtration of the sample after the titration using preweighed filters, followed by overnight drying at 105 °C and weighing.

Determination of Total Charge: To determine the amount of acid groups present after the sulfonation, the total charge of the pulp sample was measured using conductometric titration.[44] As no carboxylic groups are introduced in the functionalization route, the total charge should correspond to sulfonic acid groups introduced at the sulfonation.

A Titrino automatic conductometric titrator (Metrohm) was used to perform the titration with 0.1 M NaOH as the titrant. Prior to the titration, the sample was converted to proton form by leaving the fibers to ion exchange in 1 M HCl by 10 times for 30 min. The pH was kept around 1, to ensure that all acid groups in the sample would be protonated. After the protonation step, the sample was washed with deionized water to a conductivity of below 5 µS cm^{-1}. To prepare the sample for titration, 10 mL of 0.1 M NaCl was added to approximately 0.5 g of fibers, and then diluted to 500 mL by water. To ensure a steady flow of gas, nitrogen was bubbled through the solution for 15 min before starting the titration. The titration results in a V-shaped curve for strong acid groups, where the amount of titrant corresponding to the point of inflection of the curve can be used to calculate the total acid group content of the sample. This number is normalized to the exact dry weight of fibers in the sample as determined in the same way as described above.

Scanning Electron Microscopy-Energy Dispersive Spectroscopy (SEM-EDS): A Jeol JSM-7900F low vacuum scanning electron microscope equipped with an Oxford Instruments X-Max EDS detector was used to study the surface morphology of the sulfonated cellulose films.

Atomic Force Microscopy (AFM): AFM was used to study the surface morphology of the sulfonated cellulose films at the nanoscale. The micrographs were obtained with a Veeco Dimension 3100 microscope (Bruker, USA), using tapping mode under ambient conditions.

Liquid–Liquid Displacement Porometry: The average open pore size of the sulfonated cellulose membrane was measured using liquid–liquid displacement porometry with isobutanol and water as wetting and displacement liquids, respectively. This measurement was performed with the Porometer POROLIQ1000mL (POROMETER, Belgium) with a pressure range of 0–35 bar, which can detect pore sizes in the range 0.5 µm – 2 nm.

Brunauer-Emmett-Teller (BET) Porosity: The pore structure of sulfonated cellulose membrane was additionally studied by nitrogen sorption BET. Physical sorption measurements were carried out using a Micromeritics ASAP 2020 analyzer via N2 as adsorbent at −196 °C. The samples were degassed at 110 °C for 6 h under vacuum before analysis.

Mechanical Properties of Films: The mechanical properties of the sulfonated cellulose membranes were studied using a Zwick Z005 tensile test machine (ZwickRoell, Germany) with a pneumatic clamping system (1 kN), Xforce P load cell (1 kN), and rubber plates with large contact area toward the specimen (Vulkollan smooth 30 × 60 mm). The distance between the clamps in the setup, corresponding to the part of the sample subjected to the test, is 30 mm. Rectangular test pieces of 6 × 40 mm were prepared from the cellulose membranes using an automatic sample press in combination with a set of cutting blades of the correct dimensions. The preparation of test pieces may introduce small defects causing some samples to break at the weakened point, which may increase the variability of the results. The dry membranes were conditioned in a controlled environment of 23 °C and 50% RH for 24 h prior to the measurements. The grammage of the membranes was determined by weighing prior to the measurements. For determination of wet state mechanical properties, a membrane was equilibrated in deionized water for 24 h prior to the measurements. Any excess water on the membrane surface was removed carefully using blotting paper. A strain rate of 30 mm min^{-1} was used for all measurements.

Membrane Resistance: A symmetrical H-cell (inset Figure 2A; Scribner Associates Inc., USA) was used. The membranes were held in place using rubber o-rings and a pinch clamp. The symmetrical configuration with respect to the membrane in electrolyte solution (0.5 M KCl) of two counter electrodes (Pt/Nb mesh cylinders) and two references electrodes (two Luggin probes with reference electrodes (Ag/AgCl (3 M KCl) as terminals) was utilized for the linear sweep voltammetry measurements (from −0.1 to 0.1 V, scan rate of 10 mV s^{-1}) to estimate the through-plane membrane resistance and corresponding ionic conductivity. The Luggin probes (the capillary openings) were positioned on ≈2 mm from both sides of the membrane. The potentials were defined with respect to the open circuit potential. The close position of Luggin probes to the membrane assures the minimization of the solution resistance with respect to the membrane resistance, which allows the accurate estimation of the last one.

Transport Numbers: The ionic selectivity of membranes was compared by obtaining transport numbers for ions from measurements of cell potentials in a concentration cell using KCl at various concentration gradients.[32] Similarly, transport number for protons in the membranes was obtained using H_2SO_4 as electrolyte.

WU: The membrane pieces were immersed in boiling water for more than 1 h to achieve a full saturation. The wet membrane weight (W_{wet}) was measured after the surface water was removed using blotting paper without applying pressure. The membranes were dried at 80 °C in an oven for more than 24 h followed by cooling in a desiccator for 30 min. Then, the dry membrane weight (W_{dry}) was measured. The WU of the membranes at room temperature was calculated according to[45]

$$\mathrm{WU}(\%) = \frac{W_{wet} - W_{dry}}{W_{dry}} \times 100$$

where W_{wet} and W_{dry} are the weights of the wet and dry membrane.

AORFB: As a potential application for the sulfonated cellulose membranes, their function as cation-selective membranes for use in redox flow batteries was investigated. A flow battery setup (C-flow 5 × 5, active area of 25 cm^2 (C-Tech Innovation Ltd., UK)) employing the organic quinone redox couples alizarin red S and tiron at concentrations of 0.025 M in 1 M H_2SO_4 as anolyte and catholyte at volumes of 30 mL, respectively, was assembled. Carbon paper (AvCarb MGL 190, FuelCellStore (TX, USA)) was used as electrodes. Graphite felt (AvCarb G200 FuelCellStore (TX, USA)) was used as diffusion layer after being hydrophilized by treatment with concentrated H_2SO_4 followed by rinsing with deionized water. The cell was run at a flow rate of 15 mL min^{-1}. Nitrogen gas was continuously supplied to the anolyte and catholyte in their respective beakers during cycling of the flow battery. A BioLogic SP200 potentiostat was used for the flow battery characterization. Properties relating to both performance and stability were measured and compared when running the cell with a sulfonated cellulose membrane as well as with Nafion 115 as a reference.

The geometry of the flow cell requires a square membrane of 7 × 7 cm. For this purpose, membranes of 20 cm diameter were prepared using Rapid Köthen as described above. From such membranes, smaller membranes of the right dimensions were cut out.

Supporting Information

Supporting Information is available from the Wiley Online Library or from the author.

Acknowledgements

The authors thank VINNOVA (Digital Cellulose Center), BillerudKorsnäs, the Knut and Alice Wallenberg foundation (KAW 2019.0604, KAW 2021.0195, WWSC), the Swedish Energy Agency (52023-1), Vetenskaprådet (2016-05990) for financial funding. The authors also thank POROMETER Application Laboratory for the measurement of porosity and Benselfelt SciArt for the illustration of the membrane.

Conflict of Interest

The authors declare no conflict of interest.

Data Availability Statement

The data that support the findings of this study are available from the corresponding author upon reasonable request.

Keywords

aqueous organic redox flow batteries, crossover, ion-selective membranes, nanocellulose

Received: May 13, 2022
Revised: June 17, 2022
Published online: July 12, 2022

[1] S. Gentil, D. Reynard, H. H. Girault, *Curr. Opin. Electrochem.* **2020**, *21*, 7.
[2] European Chemicals Agency, https://echa.europa.eu/hot-topics/perfluoroalkyl-chemicals-pfas **2022**.
[3] R. S. L. Yee, R. A. Rozendal, K. Zhang, B. P. Ladewig, *Chem. Eng. Res. Des.* **2012**, *90*, 950.
[4] S. A. Muhmed, N. A. M. Nor, J. Jaafar, A. F. Ismail, M. H. D. Othman, M. A. Rahman, F. Aziz, N. Yusof, *Energy Ecol. Environ.* **2020**, *5*, 85.
[5] Y. Zhang, Y. Zhong, W. Bian, W. Liao, X. Zhou, F. Jiang, *Int. J. Hydrogen Energy* **2020**, *45*, 9803.
[6] G. Palanisamy, T. Sadhasivam, W.-S. Park, S. T. Bae, S.-H. Roh, H.-Y. Jung, *ACS Sustainable Chem. Eng.* **2020**, *8*, 2040.
[7] S.-L. Huang, M.-L. Chen, Y.-S. Lin, *React. Funct. Polym.* **2017**, *119*, 1.
[8] J. Ye, Y. Cheng, L. Sun, M. Ding, C. Wu, D. Yuan, X. Zhao, C. Xiang, C. Jia, *J. Membr. Sci.* **2019**, *572*, 110.
[9] M. Yue, Y. Zhang, L. Wang, *J. Appl. Polym. Sci.* **2013**, *127*, 4150.
[10] E. Lizundia, D. Kundu, *Adv. Funct. Mater.* **2021**, *31*, 2005646.
[11] A. Olszewska, P. Eronen, L.-S. Johansson, J.-M. Malho, M. Ankerfors, T. Lindström, J. Ruokolainen, J. Laine, M. Österberg, *Cellulose* **2011**, *18*, 1213.
[12] A. Isogai, T. Saito, H. Fukuzumi, *Nanoscale* **2011**, *3*, 71.
[13] R. Pan, O. Cheung, Z. Wang, P. Tammela, J. Huo, J. Lindh, K. Edström, M. Strømme, L. Nyholm, *J. Power Sources* **2016**, *321*, 185.
[14] A. Mukhopadhyay, Z. Cheng, A. Natan, Y. Ma, Y. Yang, D. Cao, W. Wang, H. Zhu, *Nano Lett.* **2019**, *19*, 8979.
[15] M. M. Pérez-Madrigal, M. G. Edo, C. Alemán, *Green Chem.* **2016**, *18*, 5930.
[16] T. Bayer, B. V. Cunning, R. Selyanchyn, M. Nishihara, S. Fujikawa, K. Sasaki, S. M. Lyth, *Chem. Mater.* **2016**, *28*, 4805.
[17] O. Selyanchyn, R. Selyanchyn, S. M. Lyth, *Front. Energy Res.* **2020**, *8*, 596164.
[18] H. Liimatainen, M. Visanko, J. Sirviö, O. Hormi, J. Niinimäki, *Cellulose* **2013**, *20*, 741.
[19] J. Zhang, N. Jiang, Z. Dang, T. J. Elder, A. J. Ragauskas, *Cellulose* **2008**, *15*, 489.
[20] T. Nypelö, B. Berke, S. Spirk, J. A. Sirviö, *Carbohydr. Polym.* **2021**, *252*, 117105.
[21] S. Pan, A. J. Ragauskas, *Carbohydr. Polym.* **2014**, *111*, 514.
[22] I. Rocha, N. Ferraz, A. Mihranyan, M. Strømme, J. Lindh, *Cellulose* **2018**, *25*, 1899.
[23] H. Liimatainen, J. Sirviö, O. Sundman, O. Hormi, J. Niinimäki, *Water Res.* **2012**, *46*, 2159.
[24] L. Yue, Y. Xie, Y. Zheng, W. He, S. Guo, Y. Sun, T. Zhang, S. Liu, *Compos. Sci. Technol.* **2017**, *145*, 122.
[25] T. Bayer, B. V. Cunning, B. Šmíd, R. Selyanchyn, S. Fujikawa, K. Sasaki, S. M. Lyth, *Cellulose* **2021**, *28*, 1355.
[26] J. Erlandsson, T. Pettersson, T. Ingverud, H. Granberg, P. A. Larsson, M. Malkoch, L. Wågberg, *J. Mater. Chem. A* **2018**, *6*, 19371.
[27] L. J. Small, H. D. Pratt, T. M. Anderson, *J. Electrochem. Soc.* **2019**, *166*, A2536.
[28] M. Henriksson, L. A. Berglund, P. Isaksson, T. Lindström, T. Nishino, *Biomacromolecules* **2008**, *9*, 1579.
[29] The Chemours Company FC, LCC **2016**, *Product Bulletin P-12: Nafion N115, N117, N1110 (Ion Exchange Materials Extrusion Cast Membranes)*.
[30] J. M. Sanz, D. Jardines, A. Bottino, G. Capannelli, A. Hernández, J. I. Calvo, *Desalination* **2006**, *200*, 195.

[31] J. Kamcev, R. Sujanani, E.-S. Jang, N. Yan, N. Moe, D. R. Paul, B. D. Freeman, *J. Membr. Sci.* **2018**, *547*, 123.
[32] PHYWE Systems Gmbh., *Diffusion Potentials/Nernst Equation*, PHYWE Series of Publications, 37070 Göttingen Germany **2003**.
[33] T. Sata, *Ion Exchange Membranes: Preparation, Characterization, Modification and Application*, Royal Society of Chemistry [Distributor] RSC Distribution Services, Cambridge **2004**.
[34] J. Shrawder, I. A. Cowperthwaite, *J. Am. Chem. Soc.* **1934**, *56*, 2340.
[35] R. Holze, in *Electrochemistry* (Ed: M. D. Lechner), Springer Berlin Heidelberg, Berlin, Heidelberg **2016**, pp. 1859–1862.
[36] N. Lakshminarayanaiah, *Chem. Rev.* **1965**, *65*, 491.
[37] P. Symons, *Curr. Opin. Electrochem.* **2021**, *29*, 100759.
[38] M. Vagin, C. Che, V. Gueskine, M. Berggren, X. Crispin, *Adv. Funct. Mater.* **2020**, *30*, 2007009.
[39] M. A. F. Robertson, H. L. Yeager, *Macromolecules* **1996**, *29*, 5166.
[40] C. Korzeniewski, E. Adams, D. Liu, *Appl. Spectrosc.* **2008**, *62*, 634.
[41] K. M. Cable, K. A. Mauritz, R. B. Moore, *Chem. Mater.* **1995**, *7*, 1601.
[42] C. Spiegel, *Designing & Building Fuel Cells*, McGraw Hill Professional, New York **2011**.
[43] P. A. Larsson, M. Gimåker, L. Wågberg, *Cellulose* **2008**, *15*, 837.
[44] S. Katz, R. P. Beatson, A. M. Scallan, *Sven. Papperstidn.* n.d., *1984*, 48.
[45] J.-D. Kim, S. Matsushita, K. Tamura, *Polymers* **2020**, *12*, 1354.